

FRACTURE BEHAVIOUR OF BASALT AND STEEL FIBRE REINFORCED CONCRETE

Marta KOSIOR-KAZBERUK*, Julita KRASSOWSKA

Faculty of Civil and Environmental Engineering, Białystok University of Technology, Wiejska 45E, 15-351 Białystok, Poland

Abstract: The pre-peak and post-peak softening behaviour of fine grained concrete with steel fibres and basalt fibres were investigated. The load-crack mouth opening displacement and load-deflection relationships, obtained in three-point bending test for specimens with U-notches, were used to analyze the fracture behaviour as well as to calculate the fracture energy. The strength properties of concretes tested were also compared. The modification of fracture plots, recorded under load, indicated the capability of basalt fibres to resist crack propagation. The incorporation of steel fibres caused considerable increase in fracture energy resulting in much more ductile behaviour of concrete in comparison to basalt fibre concrete. The differences in fracture behaviour of both type fibre reinforced concretes were pointed out.

Key words: concrete, basalt fibre, steel fibre, pre-peak and post-peak behaviour, fracture energy, residual flexural strength.

1. Introduction

Fibre reinforced concrete has gained increasing significance over the past years, both in research and more recently in the construction industry. Especially the precast concrete industry makes use of the special characteristics of mainly fibre reinforced concrete to reduce the weight of concrete structures producing slender and light prefabricated concrete elements (Yoo et al., 2013). Besides the non-structural elements, fibre reinforcement is particularly appealing for large structural elements. Here, steel fibres may be successfully adopted in substitution, at least partially, of the conventional reinforcement (bars or welded mesh) to reduce labour costs (Sorelli et al., 2006). Also the reduction and elimination of shear reinforcement by adding steel fibres is a common approach (Garas et al., 2012). In the recent years, important efforts have been devoted to develop new types of non-metallic fibres (Kalpokaitė Dičkuvienė et al., 2013; Sim et al., 2005; Zhang et al. 2013).

However, the full potential of fibre reinforced concrete is still not fully exploited in practice. This is mainly due to a lack of specific rules for fibre reinforced concrete in building codes. The existing rules for conventional concrete can hardly be adopted for fibre reinforced concrete that is markedly non linear since fibres start working after cracking of the concrete matrix. While conventional reinforced concrete keeps a reasonable linear behaviour until the bar yield, fibre reinforced concrete has a noticeable non linear response and, depending on the fibre content and type, fibre reinforced concrete

has a quite complicated post-cracking softening behaviour (Buratti et al., 2011; Soutsos et al., 2012). Thereby fibres ensures a significant improvement of the post-cracking behaviour and provide a high degree of ductility within the brittle cement matrix and considerable increase in the fracture energy. The latter defines the work capacity up to the total failure of the material that is frequently considered to estimate the resistance of concrete to tensile stress. Fracture energy has been implemented in the mathematical models of various finite-element-programmes for non-linear modelling. Nevertheless, specific data concerning this material parameters that would provide advancement of the material models used and subsequently the calculated structural behaviour is hardly available (Voit and Kirnbauer, 2014).

The modelling of the behaviour, damage and fracture processes of concrete is extensively discussed in the literature (Karihaloo, 2003; Kosior-Kazberuk, 2013; Shah et al., 1995). The fracture mechanics, as one of the most significant field of science, is widely used to analyze the material behaviour in structure. (Bažant, 2002). The fracture mechanics parameters are used in different applications to formulate the classic criteria of failure as well as in advanced computational methods to analyze the structures made of concrete and other brittle materials.

The main purpose of the fibres is to provide a control of cracking and to increase the fracture toughness of the brittle matrix through bridging action during both micro and macrocracking of the matrix. Debonding, sliding and pulling-out of the fibres are the local mechanisms that control the bridging action (Kazemi

* Autor odpowiedzialny za korespondencję. E-mail: m.kosior@pb.edu.pl

et al., 2007; Shah et al., 1995). The resultant composite concrete can have considerable ductility, often termed “toughness”. The ductility characteristic is dependent on fibre type, dosage, tensile strength and anchorage mechanism.

The wire steel fibres are the most common type used in non-structural and structural applications. As generally known, steel fibres continue to carry stresses after matrix failure. The additions of the most types of steel fibres do not change considerably the compressive strength and the modulus of elasticity of concrete but has noteworthy influence on the flexural strength and residual tensile strength. Thus, the analysis of post-peak responses of steel fibre reinforced concrete is crucial. The detailed information about physical and mechanical properties of steel fibre reinforced concrete can be found for example in (Bordelon, 2007; Michels et al., 2013; Sorelli et al., 2006). The most of current experiments relate to concrete reinforced by steel fibres and very few present the research on composites with other kinds of fibres i.e. basalt fibres, which can offer the series of advantages.

Usually, the steel fibres are stiff and, in order to gain pull-out resistance, they have enlarged, flattened or hooked end, roughened surface texture or wavy profiles. They vary in length up to about 60 mm, with aspect ratios (ratio of length to nominal diameter) from 20 to 100.

In contrast, the basalt fibres are much more slender and soft in comparison to steel fibres. The typical length range is from 12 to 54 mm and the diameter range is from 9 to 20 mm. Basalt fibres are obtained from basalt rocks through melting and drawing process. Therefore, the fibre has inherited the basalt ore structure and performance characteristics, such as outstanding thermal stability, anti-corrosive performance, ideal heat insulation, sound absorption, and low moisture absorption. In addition, this fibre exhibits high strength and high module performance. It is known that the basalt fibres have better tensile strength than the E-glass fibers, greater failure strain than the carbon fibers as well as good resistance to chemical attack, impact load and fire (Sim et al., 2005; Di Lodovico et al., 2010). However, previous studies on the use of basalt fibres in concrete are limited. Sim et al. (2005) investigated the properties of concrete containing continuous basalt fibre. The results show improvement in the thermal and mechanical properties of concrete. Limited research has studied the effect of short basalt fibre on the mechanical properties of geopolymeric concrete (Dias and Thaumaturgo, 2005; Li and Xu, 2009) and mechanical and thermal features (Borhan, 2012). Kabay (2014) reported that the addition of short basalt fibers resulted in decrease in compressive strength and at the same time the enhancement of fracture energy and reduction of abrasive wear of concrete. Therefore further experimental studies should be conducted on the use of basalt fibre in cement based composites to characterize its effects on physical and mechanical properties of composites.

Model Code 2010 (2012), RILEM TC 162 (2002, 2003) and ACI 544 (1998) provide guidelines to designers

of concrete structures. However, on a practical level, current design codes for structures do not usually cover fibre reinforced materials and designers hardly accept the volunteering guidelines or research results available in scientific papers. For this reason, further research on concretes with various types of fibre is still needed to confirm their advantages, particularly the flexural toughness and fracture energy which are used for design purposes.

The aim of the research work was the investigation of the fracture behaviour of fine grained concrete with basalt fibres and steel fibres. The fibres of the same length ($l = 50$ mm) but different shape and properties were chosen for tests. The characteristics of concretes with fibres were determined in three-point-bending test on notched beam specimens.

2. Experimental program

2.1. Materials and specimens preparation

The tests were performed on fine grained cement concrete. The cement (CEM I 42,5 R) content was constant – 320 kg/m³ and the water to cement ratio of 0,50 were kept constant in all mixes. The river sand, fraction 0-2 mm and the natural aggregate with maximum diameter of 4 mm were used. The maximum size of aggregate was limited to reduce its influence on fracture properties and to provide the homogenous fibres distribution in concrete. The minimum size of specimen exceeded the maximum size of aggregate more than tenfold.

The polycarboxylate polymer based superplasticizer was used to minimize fiber clumping and enhance fiber dispersion in concrete mix. The superplasticizer was applied in the amount of 0,6% of cement mass. Table 1 gives the mix proportions for reference concrete.

Tab. 1. Mix proportions of the reference concrete.

Component	Dosage (kg/m ³)
Cement CEM I 42,5 R	320
Aggregate 0-2 mm	1326
Aggregate 2-4 mm	624
Water	160
Superplasticizer	1.92

The fibres were added into concrete as a replacement of an adequate portion of aggregate by volume. Two fibre types were used to study the concrete strength properties and post-crack behaviour: the hooked end, circular cross-section steel fibres and chopped basalt fibres. The geometry and parameters of both types of fibres are presented in Table 2. Three different volume fractions of steel fibres were applied to cover the majority of practically used fraction range: 0.5%, 1.0% and 1.5%, which was the dosage of 40, 80 and 120 kg/m³, respectively. The basalt fibres were added at three

contents of 1.0, 2.5 and 5.0 kg/m³, which gave volume fractions 0.038%, 0.095% and 0.19%, respectively. The content of basalt fibres suggested by manufacturer is 2.0 kg/m³.

Tab. 2. Properties of fibres used.

Property	Steel fibres	Basalt fibres
Fibre shape	hooked end	straight
Length (mm)	50	50
Diameter (mm)	1.0	0.02
Tensile strength (MPa)	900	1680
Elastic modulus (GPa)	200	89
Density (kg/m ³)	7850	2660

The dry aggregate was mixed with fibres followed by cement. The materials were dry mixed for 2 min before adding the water with superplasticizer. Mixing continued for a further 4 min. The time of mixing was considered sufficient for the proper dispersion of fibres in the mix without causing a "balling" effect.

The notched beams of size 100×100×400 mm were used for three-point bending test. The initial saw-cut notch with a depth equal to 30 mm and width of 3 mm was located in the mid-span place. The geometry of specimen and the way of load were presented in Fig. 1. The elongated U-notches ($a_0 / d = 0.30$) were sawn under wet conditions one day before the test. Each series was composed of 4 replicates.

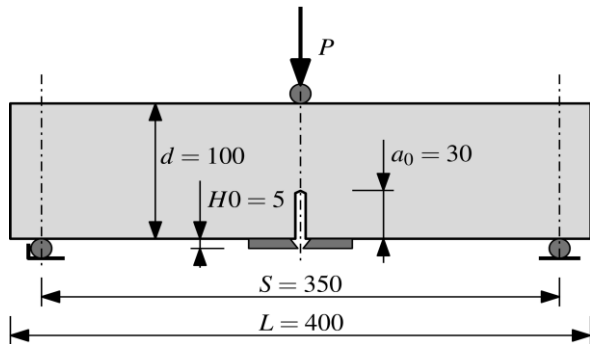


Fig. 1. Fracture testing configuration and geometry of specimen with elongated U-notch.

Moreover, for each fibre dosage three beams (100×100×400 mm) for flexural strength were also cast and four cubes (100×100×100 mm) for the compressive strength were cut from beam specimens.

The specimens were vibrated in moulds and then stored under polyethylene cover for one day. After demoulding all specimens were cured in water at the temperature of 20±2°C till they were tested.

2.2. Test procedures

A three-point bending method was used to determine the fracture performance of concretes with fibres and control

concrete without reinforcement in accordance with the recommendation of RILEM Fracture Mechanics Committee (TC50-FMC, 1985) and EN 14651 (2005).

The universal testing machine (MTS 322) with closed-loop servo control was used to achieve a stable failure of specimens. The crack mouth opening displacement (CMOD) measured at the center of the notch was a feedback signal. The clip gauge was used to measure the CMOD values. The load-deflection ($P-\delta$) curves and load – crack mouth opening displacement (P -CMOD) were determined for fracture behaviour analysis. At the same time the complete load-time cure was recorded to check the test stability. Fig. 2 shows the universal testing machine with beam specimen and clip gauge.



Fig. 2. Notched beam specimen during testing.

The fracture energy (G_F) is defined as the area under the load-deflection curve per unit fractured surface area and since no energy dissipation is assumed to take place at the crack tip, this area can be associated with the fracture energy:

$$G_F = \frac{\int_0^{\delta_{\max}} P(\delta) d\delta + mg\delta_{\max}}{(d - a_0)b} \quad (1)$$

where: $g = 9,81 \text{ m/s}^2$, d – beam depth, b – beam width, a_0 – notch depth and d_{\max} – maximum deflection. In connection with the test, the weight of the beam m was determined and included into calculation of G_F .

The secant elastic modulus were calculated from load-displacement relationship. The flexural strength was defined by the load capacity at the first crack in three-point bending test. Compressive strength of concrete was determined according to EN 12390-3 (2011).

3. Analysis of test results

3.1. Fracture behaviour of basalt fibre reinforced concrete

The fracture behaviour was analysed on the basis of P -CMOD curves and $P-\delta$ curves obtained for concrete specimens. The characteristic load P plotted versus

CMOD and P versus the deflection in the mid-span δ measured for concretes with basalt fibres were presented in Figs. 3 and 4, respectively.

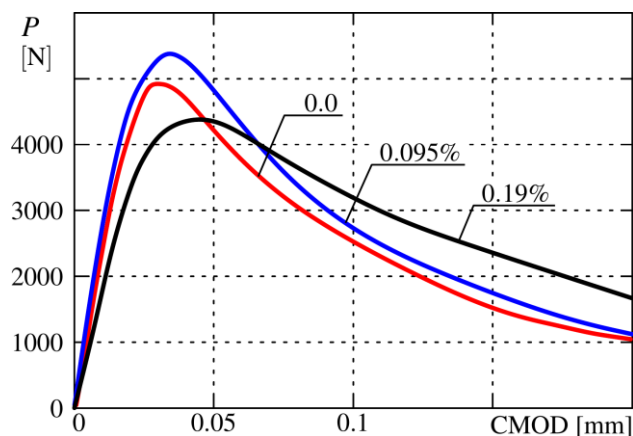


Fig. 3. Load P versus CMOD curves for concretes with various volume fractions of basalt fibres.

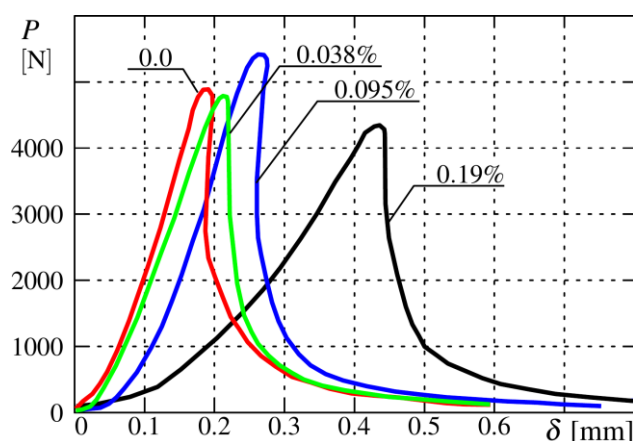


Fig. 4. Load P versus deflection δ diagrams of concretes with various volume fractions of basalt fibres.

The analysis of P -CMOD plots for concretes with basalt fibres makes it possible to investigate the changes in concrete properties related to the loss of brittle material character. From the P -CMOD diagram, one can see that the initial parts of the curve for all concretes considered are almost linear and the strain of the notch tip under tension increases slightly with the increasing load. After the linear segment of P -CMOD curve, deviation from linear response is observed and the load reaches the maximum value, which indicates the onset of crack initiation at the tip of the notch. The increase in basalt fibre content cause the increase in the length of segment until reaching the peak. The crack mouth opening displacement, recorded for maximum load for individual specimens, increased when the content of fibre increased. Generally, the $CMOD_{max}$ values for fibre reinforced concrete were greater than recorded for control concrete specimens. However, the influence of basalt fibre content on the maximum load is not clear. The addition of fibre up to 0.095% (2.5 kg/m³) caused the increase in P_{max} , but further increase in fibre content up to 0.19% (5.0 kg/m³) caused the decrease in maximum load value.

The post-critical part of P -CMOD curve was also influenced by content of fibres in concrete. For reference concrete the clear force drop and the strain softening behaviour were observed. For concretes with basalt fibres, the general tendency was similar, but the fibres allow transferring higher stress at large crack openings. The load decreased much slower for specimens of fibre concrete.

As can be seen from Fig. 4, there is an increasing tendency in the deflection δ_{max} in span center, recorded for P_{max} , with the increase in fibre content.

As can be found in Fig. 4, the incorporation of the basalt fibre does influence not only the post-peak behavior of concrete beam but also the pre-peak part of load-deflection curve. The comparison of ascending and descending part of load- δ diagrams for concretes with different basalt fibre dosage indicated the significant fibre influence on ascending part connected with microcrack formation and localization. To give an idea about the relative and absolute proportion of the fracture energy, Table 3 illustrates the portion of energy until crack propagation (up to achieve the breaking load P_{max} and δ_{max}) related to the total measured energy G_F . The energy demand necessary for crack initiation increased gradually with the increase in fibre volume fraction. It may be concluded that both elastic and plastic portions of energy increased. The detailed analysis of basalt fibre influence on ascending and descending part of load-deflection diagram and on variations of fracture energy was presented by Kosior-Kazberuk and Krassowska (2015).

Tab. 3 Total fracture energy G_F and portion of energy until crack propagation $G_F(\delta_{max})$ determined for specimens with basalt fibres.

Basalt fibre content (% vol.)	G_F (Nm/m ²)	$G_F(\delta_{max})$ (Nm/m ²)	$G_F(\delta_{max})$ (%)
0	98	40	41
0.038	116	49	42
0.095	133	73	55
0.190	171	99	58

The basalt fibres help to limit the generation of cracks. When the stress is transferred to the basalt fibre from cement matrix, the fibre can restrict the crack from developing. The crack continues to develop only by bypassing the fibre or pulling very thin fibre to be broken, during the course of which, an additional amount of energy is consumed. The larger fibre dosage causes the stronger restriction of fibre, and as the result the increase in fracture energy.

3.2. Fracture behaviour of steel fibre reinforced concrete

The characteristic load P plotted versus CMOD and P versus the displacement in the mid-span d measured for concretes with steel fibres were presented in Figs. 5 and 6, respectively.

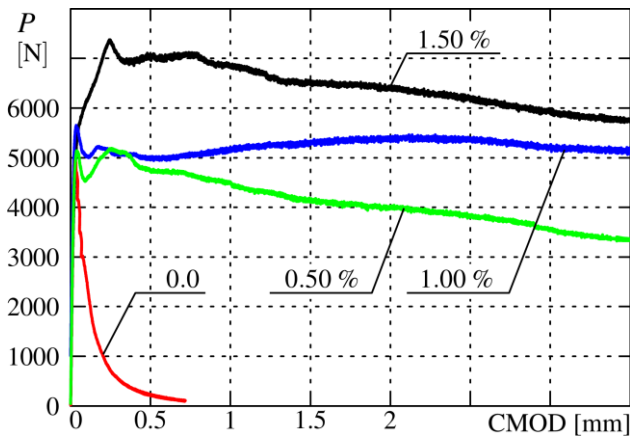


Fig. 5. Load P versus CMOD curves for concretes with various volume fraction of steel fibres.

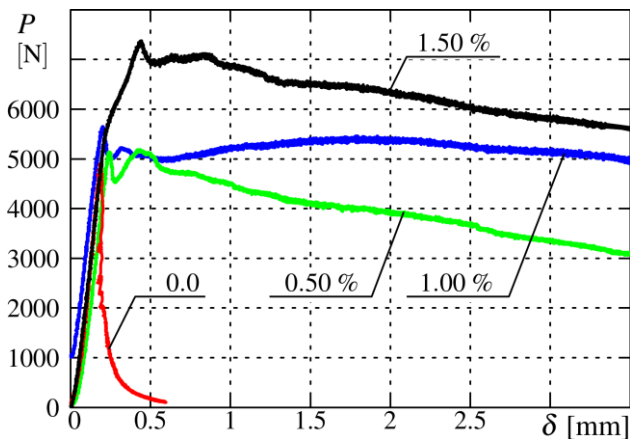


Fig. 6. Load P versus deflection δ of concretes with various volume fractions of steel fibres.

The influence of steel fibre addition expresses itself by reaching a higher maximum ultimate load, larger displacement, and thus a larger area under the load-displacement curve and consequently considerable greater fracture energy resulting in much more ductile behaviour of concrete. In a typical load vs. CMOD diagram of a specimen under three-point loading, the material exhibits linear behaviour up to its first crack stress (well marked first peak), a post-first-crack strain hardening phase up to its ultimate flexural load, and a post-ultimate-load phase. The descending parts of diagrams for concretes with different fibre dosage are characterized by apparent nonlinearity and significant scatter of test results. Both the strain softening and hardening were observed.

The hooked end steel fibres are typical example of “slipping fibres”. When a crack opens, the “slipping fibres” slip and never break. The stress transfer across the crack surfaces was closely related to the fibres debonding and pulling out. As microcracks grow and join into larger macrocracks, the long hooked-end fibres become more and more active in crack bridging. This type of fibres provide a very long plateau of post-crack residual strength (Vandewalle, 2008; Köksal et al., 2013).

The residual flexural tensile strength $f_{R,i}$, which is an important parameter characterising the post-cracking

behaviour of steel fibre reinforced concrete was determined on the basis of P -CMOD diagrams. The residual strengths $f_{R,1}$, $f_{R,2}$, $f_{R,3}$ and $f_{R,4}$ respectively, were defined at the following CMODi: 0.5; 1.5; 2.5; 3.5 mm according to RILEM TC 162-TDF (2002) and EN14651 (2005) and presented in Table 4. The residual strength is a parameter considered in guidelines for concrete structure design (Model Code, 2012; RILEM TC 162-TDF, 2003) The hooked-end steel fibre are very effective in improving the post-peak parameters. The deformed shape provides better bond conditions. Of course, the residual strength is higher when the higher amount of fibre is added to the concrete mix and the variations of $f_{R,i}$ depend on the fibre content in concrete. In case of concrete reinforced with 0.5% of fibre the post-peak part of the load-CMOD diagram drops down while for higher fibre dosages it decreases very slowly. Vandewalle (2008) confirmed that the origin of the higher residual strength for long hooked-end fibres at larger CMOD values is twofold: presence of a hooked-end and long embedded length.

Tab. 4. Residual flexural strength of steel fibre reinforced concretes.

Parameter	CMOD (mm)	Steel fibre content (% vol.)		
		0.50	1.00	1.50
f_{R1} (MPa)	0.5	3.48 (0.42)	4.50 (0.41)	6.92 (0.53)
f_{R2} (MPa)	1.5	3.05 (0.36)	4.37 (0.32)	6.55 (0.57)
f_{R3} (MPa)	2.5	2.52 (0.35)	4.26 (0.49)	5.94 (0.41)
f_{R4} (MPa)	3.5	1.76 (0.26)	3.95 (0.39)	5.50 (0.51)

Standard deviations of the test results are presented in brackets.

Regarding the fracture energy G_F is the product of load and deflection, the variations of P - δ diagrams (Fig. 6) reflects the variations of G_F . In general, the concrete beam specimens containing steel fibres had higher energy absorption capacity that the plain concrete beam specimens. However, the energy absorption at the maximum load (area under the load-deflection curve) is almost similar for plain concrete specimens and specimens containing 0.5% and 1.0% of steel fibre. The added steel fibres have significant effect on total energy absorption (Table 5). Fig. 7 shows the average dissipated energy G_F versus CMOD for concretes containing steel fibres. The growth of G_F is linear and the differences in energy values, determined for particular volume fraction of fibres, become greater and greater when CMOD value increases.

Tab. 5. Mechanical properties of concretes with both sorts of fibres.

Sort of fibre	Fibre content (% vol.)	Compressive strength (MPa)	Elastic modulus (MPa)	Flexural strength (MPa)	Maximum load (N)	Max. load deflection (mm)	Total fracture energy (Nm/m ²)
non	0	53.0 (3.8)	28590 (1870)	3.53 (0.6)	4900 (110)	0.18	98 (5.8)
Basalt fibre	0.038	56.8 (2.0)	29775 (2322)	3.69 (0.3)	4930 (198)	0.22	116 (3.0)
	0.095	58.6 (0.9)	33500 (1940)	3.94 (0.2)	5570 (167)	0.26	133 (7.4)
	0.190	52.9 (4.2)	32830 (2310)	3.60 (0.4)	4850 (210)	0.42	171 (10.1)
Steel fibre	0.50	54.4 (2.3)	29860 (1560)	3.76 (0.3)	5240 (144)	0.20	1050 (80)
	1.00	55.1 (2.8)	30530 (2430)	5.49 (0.8)	5800 (169)	0.34	1930 (105)
	1.50	58.0 (1.7)	32110 (3208)	7.53 (1.1)	7050 (246)	0.45	2758 (206)

Standard deviations of the test results are presented in brackets.

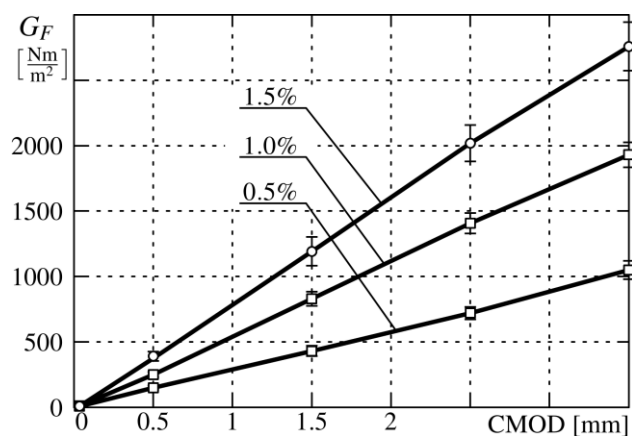


Fig. 7. Dissipated energy G_F versus CMOD for concretes with steel fibres.

3.3. Properties of fibre reinforced concrete

Mechanical properties of concretes containing two significantly different types of fibres were given in Table 5.

Basalt fibers improved the fracture toughness of concrete significantly, but these fibers had very little effect on strength characteristics of concrete. It should be marked that fibers do not significantly influence flexural tensile strength, as defined by the load capacity at first crack. The increases in both the flexural and compressive strength of basalt fibers were insignificant. The addition of fiber up to 0.19% (5 kg/m³) caused the slight reduction in compressive strength. Similar effect of higher dosage of basalt fibers was observed by Kabay (2014). The incorporation of fibers did not significantly improve the modulus of elasticity. The most significant changes in comparison to reference concrete were observed for fracture energy. The total fracture energy of concrete containing 0.19% of basalt fibres increased almost twice in comparison to the reference concrete without fibers. The deflection recorded for maximum load increased with the increased dosage of fibers, although the value of maximum load did not change significantly.

The incorporation of steel fibres, in considered volume fractions, had very slight influence on the compressive strength and modulus of elasticity, but steel fibres

appeared to increase the flexural strength almost twice (for concrete containing 1.5% of fibres) in comparison to reference concrete (see Table 5). The values of maximum load and the corresponding deflections increased with the fibre dosage increase. The total fracture energy depended on the fibre dosage and it achieved the values many times greater than fracture energy determined for basalt fibre reinforced concretes and reference concrete.

4. Conclusions

The influence of two different types of fibres on the fracture behaviour of cement concrete was analysed. The reference fine grained concrete was modified by incorporation of various dosages of basalt and steel fibres. There was showed that the load-CMOD and load-deflection curves, recorded in three-point bending test, can take quite different shapes depending on the geometry and mechanical properties of fibres. The influence of fibres is in enhancing the resistance to crack propagation resulting in an increase in composite toughness and it could be determined from load-CMOD or load-deflection measurement. Both types of fibres tested influence the fracture behaviour of concrete, but their effect on pre-peak and post-peak performance is different.

The incorporation of considered volume fraction (0.038-0.19%) of thin, soft basalt fibres had an influence on the fracture properties of concrete, while the fibers had a slight effect on the strength properties of concrete. The improvement of pre-peak and post-peak behavior was observed. The results of measuring the toughness and energy-absorption characteristics of fiber reinforced concrete, demonstrated that basalt fibres concrete specimens acquire better ductile behavior and energy absorption capacity, compared to ordinary concrete specimens. The variation in fracture parameters and the modifications of fracture curves, recorded under load, indicate the capability of the basalt fibres to resist crack propagation. Such significant changes in concrete behaviour should be taken into account in modelling and design of structures.

The stiff, hooked-end steel fibres (incorporated in the volume fraction of 0.5-1.5%) influenced concrete performance more efficiently than basalt fibres. The flexural tensile strength and the ductility increased with increasing fibre volume as expected. Steel fibres had relatively slight effect on pre-peak behaviour of concrete specimens. These parts of load-CMOD or load-deflection plot were more linear in comparison to plots obtained for basalt fibre reinforced concrete. In this phase the steel fibres were particularly effective in the elimination of influence of pores and other microstructure defects on concrete specimen behaviour under load. The stable post-peak performance at larger CMOD values was dominated by the volume of steel fibres due to the presence of the hooks and its large embedded length.

References

- ACI 544. IR-96 (1998). State-of-the-art report on fibre reinforced concrete. Manual of concrete practice. Farmington Hills.
- Bazant Z.P. (2002). Concrete fracture models: testing and practice. *Engineering Fracture Mechanics*, Vol. 69, 165-205.
- Bordelon A.C. (2007). Fracture behavior of concrete materials for rigid pavements system. MA Thesis. Graduate College of University of Illinois at Urbana-Champaign, USA.
- Borhan T.M. (2012). Properties of glass concrete reinforced with short basalt fibre. *Materials and Design*, Vol. 42, 265-271.
- Buratti N., Mazzotti C., Savoia M. (2011). Post-cracking behaviour of steel and macro-synthetic fibre-reinforced concretes. *Construction and Building Materials*, Vol. 25, 2713-2722.
- Dias D., Thaumaturgo C. (2005). Fracture toughness of geopolymeric concretes reinforced with basalt fibers. *Cement & Concrete Composites*, Vol. 27, No. 1, 49-54.
- Di Lodovico M., Prota A., Manfredi G. (2010). Structural upgrade using basalt fibres for concrete confinement. *Journal of Composites for Construction*, Vol. 14, No. 5, 541-552.
- EN 12390-3 (2011). Testing hardened concrete: Compressive strength of test specimens.
- EN 14651 (2005). Test method for metallic fibered concrete – measuring the flexural tensile strength.
- Garas V.Y., Kurtis K.E., Kahn L.F. (2012). Creep of UHPC in tension and compression: effect of thermal treatment. *Cement & Concrete Composites*, Vol. 34, No. 4, 493-502.
- Kalpokaitė Dičkuviene R., Lukošiuūtė I., Brinkienė K., Baltušnikas A., Čėsniene J. (2013). Applicability of the waste fibres in cement paste. *Materials Science (Medžiagotyra)*, Vol. 19, No. 3, 331-226.
- Kabay N. (2014). Abrasion resistance and fracture energy of concretes with basalt fiber. *Construction and Building Materials*, Vol. 50, 95-101.
- Karihaloo B.L. (2003). *Failure of concrete*, in: *Comprehensive structural integrity*, Elsevier Pergamon, UK, 477-548.
- Kazemi M.T., Fazileh F., Ebrahiminezhad M.A. (2007). Cohesive crack model and fracture energy of steel-fiber-reinforced-concrete notched cylindrical specimens. *Journal of Materials in Civil Engineering*, Vol.19, No. 10, 884-890.
- Kosior-Kazberuk M. (2013). Variations in fracture energy of concrete subjected to cyclic freezing and thawing. *Archives of Civil and Mechanical Engineering*, Vol. 13, 254-259.
- Kosior-Kazberuk M., Krassowska J. (2015). Post-cracking behaviour of basalt fibre reinforced concrete. *Proc. of the 6th International Conference on Mechanics and Materials in Design*, J.F. Silva Gomes, S.A. Meguid (Eds), P. Delgada, Azores, 26-30 July 2015, 673-682.
- Köksal F., Şahin Y., Gencil O., Yiğit İ. (2013). Fracture energy-based optimisation of steel fibre reinforced concretes. *Engineering Fracture Mechanics*, Vol. 107, 29-37.
- Li W., Xu J. (2009). Mechanical properties of basalt fiber reinforced geopolymeric concrete under impact loading. *Material Science Engineering A*, Vol. 505 No. 1-2, 178-186.
- Michels J., Christen R., Waldmann D. (2013). Experimental and numerical investigation on postcracking behavior of steel fiber reinforced concrete. *Engineering Fracture Mechanics*, Vol. 98, 326-349.
- Model Code 2010 (2012). Comité Euro-International du Béton fib (CEB-FIP).
- RILEM Draft Recommendation TC 50-FMC (1985). Determination of the fracture energy of mortar and concrete by means of three-point bend tests on notched beams. *Materials and Structures*, Vol. 18, 285-290.
- RILEM TC 162-TDF (2002). Test and design method for steel fibre reinforced concrete. Bending test. Final recommendation. *Materials and Structures*, Vol. 35, 579-582.
- RILEM TC 162-TDF (2003). Test and design method for steel fibre reinforced concrete σ - ϵ design method. *Materials and Structures*, Vol. 36, 560-567.
- Shah S.P., Swartz S.E., Ouyang Ch. (1995). Fracture mechanics of concrete: Applications of fracture mechanics to concrete, rock and other quasi-brittle materials. *John Wiley & Sons, Inc.*, New York.
- Sim J., Park C., Moon D. (2005). Characteristics of basalt fiber as a strengthening material for concrete structures. *Composites Part B: Engineering*, Vol. 36, 504-512.
- Sorelli G., Meda A., Plizzari G.A. (2006). Steel fiber concrete slabs on ground: a structural matter. *ACI Structural Journal*, Vol. 103, No. 4, 551-558.
- Soutsos M.N., Le T.T., Lampropoulos A.P. (2012). Flexural performance of fibre reinforced concrete made with steel and synthetic fibres. *Construction and Building Materials*, Vol. 36, 704-710.
- Vandewalle L. (2008). Hybrid fibre reinforced concrete, In: *Harnessing fibres for concrete construction*, R.K. Dhir, M.D. Newlands, M.J. McCarthy, K. Paine (Eds), Proc. of the International Conference, University of Dundee, Scotland, UK, 10 July 2008, 11-22.
- Voit K., Kirnbauer J. (2014). Tensile characteristics and fracture energy of fiber reinforced and non-reinforced ultra high performance concrete (UHPC). *International Journal of Fracture*, Vol. 188, 147-157.
- Yoo D.-Y., Park, J.-J., Kim, S.-W., Yoon, Y.-S. (2013). Early age setting, shrinkage and tensile characteristics of ultra high performance fiber reinforced concrete. *Construction and Building Materials*, Vol. 41, 427-438.
- Zhang P., Liu Ch., Li Q., Zhang T. (2013). Effect of polypropylene fiber on fracture properties of cement treated crushed rock. *Composites: Part B*, Vol. 55, 48-54.

**ZMIANY PARAMETRÓW MECHANIKI
PĘKANIA BETONÓW ZAWIERAJĄCYCH
WŁÓKNA BAZALTOWE I STALOWE**

Streszczenie: Badano wpływ włókien bazaltowych i stalowych na podkrytyczne i pokrytyczne zachowanie się elementów próbnych z betonu drobnoziarnistego. Wykresy zależności obciążenie-rozwarcie wylotu karbu oraz zależności obciążenie-ugięcie, uzyskane w warunkach trójpunktowego zginania próbek beleczkowych z karbem typu U, wykorzystano do analizy zmian parametrów mechaniki pęknięcia oraz obliczenia energii pęknięcia. Porównano właściwości wytrzymałościowe badanych betonów. Wykazano, że beton zbrojony włóknami bazaltowymi

charakteryzuje się zwiększoną odpornością na inicjację i propagację rys. Wprowadzenie włókien stalowych do betonu spowodowało znaczące zwiększenie energii pęknięcia, a także zmianę charakteru materiału w kierunku bardziej ciągliwego w porównaniu do betonu z dodatkiem włókien bazaltowych. Wskazano istotne różnice charakterystyk pęknięcia betonów z dodatkiem obu rodzajów włókien.

Acknowledgments

The research work was financially supported by National Science Centre (Poland); project No. 2011/03/B/ST8/06456.